

Epitranscriptome sequencing technologies: decoding RNA modifications

Xiaoyu Li^{1,2}, Xushen Xiong¹⁻³ & Chengqi Yi^{2,4}

In recent years, major breakthroughs in RNA-modification-mediated regulation of gene expression have been made, leading to the emerging field of epitranscriptomics. Our understanding of the distribution, regulation and function of these dynamic RNA modifications is based on sequencing technologies. In this Review, we focus on the major mRNA modifications in the transcriptome of eukaryotic cells: *N*⁶-methyladenosine, *N*^{6,2'}-*O*-dimethyladenosine, 5-methylcytidine, 5-hydroxymethylcytidine, inosine, pseudouridine and *N*¹-methyladenosine. We discuss the sequencing technologies used to profile these epitranscriptomic marks, including scale, resolution, quantitative feature, pre-enrichment capability and the corresponding bioinformatics tools. We also discuss the challenges of epitranscriptome profiling and highlight the prospect of future detection tools. We aim to guide the choice of different detection methods and inspire new ideas in RNA biology.

More than 100 distinct chemical modifications to RNA have been characterized to date. They are present in abundant noncoding RNAs (ncRNAs)—including ribosomal RNA (rRNA), transfer RNA (tRNA) and small nuclear RNA (snRNA)—and are important for maintaining the proper functions of ncRNAs in translation and splicing. Several modifications, including *N*⁶-methyladenosine (m⁶A), 5-methylcytidine (m⁵C), inosine (I), pseudouridine (Ψ), *N*¹-methyladenosine (m¹A) and 5-hydroxymethylcytidine (hm⁵C), are found internally in eukaryotic mRNA and can influence the metabolism and function of mRNA¹ (Fig. 1). Thus, the multitude of RNA modifications together were first designated 'RNA epigenetics' in 2010 (ref. 2), and the term 'epitranscriptome' was coined in 2012 (ref. 3) in analogy to epigenetic regulation mediated by modifications to DNA and histone.

However, functional studies of the epitranscriptome lagged behind those of the epigenome on account of the lack of sensitive and robust sequencing technologies that could detect these epitranscriptomic marks in a transcriptome-wide manner. Several major challenges exist for mapping the epitranscriptome. First, the majority of

RNA modifications cannot be directly detected by high-throughput sequencing. Because chemical modifications to RNA often do not change the base pairing properties of the modified bases, reverse transcription (RT) will simply erase these modifications and render them indistinguishable from the regular RNA bases. Second, while rRNA, tRNA and snRNA are abundant, other types of cellular RNA—for instance, mRNA and long noncoding RNA (lncRNA)—can be of low abundance. Third, there is a lack of existing computational tools to facilitate the identification of modification sites from sequencing data.

Fortunately, recent years have witnessed major advances in the development of novel transcriptome-wide sequencing technologies for distinct epitranscriptomic marks. These new tools have helped researchers to identify the location of RNA modifications and to reveal these modifications' distinct distribution patterns throughout the transcriptome. When these sequencing methods are combined with other emerging tools (for instance, genome-editing tools), targets of RNA-modifying enzymes have been identified. In addition, these technologies have uncovered the dynamic nature of

¹State Key Laboratory of Protein and Plant Gene Research, School of Life Sciences, Peking University, Beijing, China. ²Peking-Tsinghua Center for Life Sciences, Peking University, Beijing, China. ³Academy for Advanced Interdisciplinary Studies, Peking University, Beijing, China. ⁴Synthetic and Functional Biomolecules Center and Department of Chemical Biology, College of Chemistry and Molecular Engineering, Peking University, Beijing, China. Correspondence should be addressed to C.Y. (chengqi.yi@pku.edu.cn).

RECEIVED 25 AUGUST; ACCEPTED 28 NOVEMBER; PUBLISHED ONLINE 29 DECEMBER 2016; CORRECTED AFTER PRINT 10 FEBRUARY 2017; DOI:10.1038/NMETH.4110

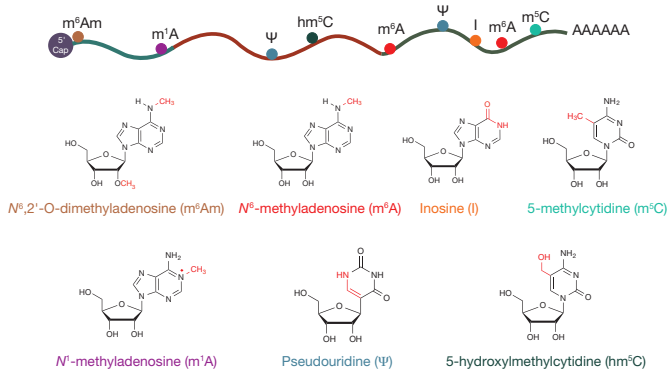


Figure 1 | Chemical modifications in mRNA.

distinct epitranscriptomic marks under different physiological conditions. Furthermore, these tools have enabled the discovery of ‘reader’ proteins that selectively recognize specific epitranscriptomic marks and determine their function. Hence, new sequencing tools not only allow comprehensive profiling of the epitranscriptome but are also valuable resources for functional epitranscriptomic investigations.

While many excellent reviews have summarized the biological functions of different epitranscriptomic marks^{4–9}, here we focus on the principles of the sequencing technologies, their bioinformatics algorithm, detection scale, resolution and ability to yield quantitative information. The stoichiometry of RNA modifications is important for assessing the extent of biological impact one modified nucleotide could have on the entire transcript. We also look at whether a given detection method is capable of pre-enrichment before sequencing, which determines the sensitivity of a sequencing method, the required sequencing depth and thus costs.

m⁶A, the first reversible mRNA modification

m⁶A is the most abundant internal mRNA modification in eukaryotes (Supplementary Table 1). It is catalyzed by a methyltransferase complex, or ‘writers’, which includes at least METTL3, METTL14 and WTAP^{10–15}. m⁶A is the first reversible RNA modification found in eukaryotic cells; it can be demethylated by FTO and ALKBH5 (termed ‘erasers’)^{16,17}. In fact, it is the discovery of the reversible nature of m⁶A that led to renewed interest in this long-known mRNA modification². In addition, multiple m⁶A-specific binding proteins (‘readers’) have been identified, and these reader proteins can affect the metabolism and function of m⁶A-marked mRNAs in various ways^{18–24}. Besides its regulatory roles in mammalian cells, m⁶A can also be installed on viral RNA and influences virus infection and production^{25–29}.

m⁶A in mRNA was first discovered in the 1970s (ref. 30); follow-up studies revealed several abundant m⁶A sites that are associated with an RRACH (R = A/G, H = U/A/C) consensus sequence^{31–33}. However, a transcriptome-wide profile of m⁶A in mammalian cells remained unclear until two groups independently developed two robust methods in 2012, both of which are based on m⁶A-specific methylated immunoprecipitation and high-throughput sequencing (m⁶A-seq¹⁹ and MeRIP-seq³⁴). In these methods, purified mRNA is fragmented to ~100–150 nt and immunoprecipitated by an m⁶A-specific antibody. The enriched m⁶A-containing RNA fragments are then subjected to library construction and high-throughput sequencing (Fig. 2a). These two methods have identified approximately 10,000 of m⁶A peaks in the mammalian transcriptome and revealed for the first time that m⁶A

peaks are enriched in 3′ UTRs and near stop codons. These methods, which have a resolution of 100–200 nt, are easily manageable; they were quickly adopted by many different laboratories and have enabled many important discoveries in the field of epitranscriptomics. Later, a modified m⁶A immunoprecipitation method of higher resolution was reported and applied to the study of yeast in meiosis³⁵. In this method, a yeast strain deficient in m⁶A methyltransferases is used as a negative control to eliminate the false-positive peaks (Fig. 2a). In addition, shorter m⁶A fragments and a ligation-based strand-specific library preparation protocol are used to increase the m⁶A detection resolution; together with the knowledge of the m⁶A consensus motif, a nearly single-base-resolution m⁶A profile in yeast is obtained. Collectively, these early methods reveal the transcriptome-wide m⁶A landscapes in eukaryotic cells and provide valuable tools for functional studies of m⁶A, which is now unambiguously established as a key epitranscriptomic mark.

Recently, UV-induced RNA-antibody crosslinking strategies have been adapted into the m⁶A-seq and MeRIP-seq protocols, allowing identification of base-resolution m⁶A methylomes in human cells. Two types of UV-crosslinking are used; the first incorporates photoactivatable ribonucleoside-enhanced crosslinking and immunoprecipitation (PAR-CLIP), hence leading to photo-crosslinking-assisted m⁶A sequencing strategy (PA-m⁶A-seq)³⁶. In this strategy, 4-thiouridine (4SU) is incorporated into RNA by adding 4SU into the growth medium. After m⁶A immunoprecipitation, the recovered m⁶A-containing RNA is crosslinked to the anti-m⁶A antibody under 365-nm UV light. The crosslinked RNA is then digested to ~30 nt using RNase T1 and subjected to sequencing (Fig. 2b). Because 4SU induces a T-to-C mutation at the site of crosslinking, PA-m⁶A-seq efficiently increases the signal-to-noise ratio of methylation detection. In addition, by combining the single consensus methylation sequences within the ~25–30 nt windows, m⁶A sites can be detected at single-base resolution. Yet, for m⁶A modifications that do not have a nearby site for 4SU incorporation, these m⁶A sites may be missed in this method. The other UV-crosslinking strategy takes advantage of crosslinking immunoprecipitation (UV CLIP), leading to m⁶A-CLIP and m⁶A individual-nucleotide-resolution crosslinking and immunoprecipitation (miCLIP), respectively^{37,38}. In m⁶A-CLIP and miCLIP, RNA fragments are immunoprecipitated and crosslinked to antibody by 254-nm UV light. Unlike m⁶A-seq, which uses competition elution to recover the m⁶A-containing RNA, both m⁶A-CLIP and miCLIP use proteinase K to retrieve the crosslinked RNA. The protein–RNA crosslinking sites lead to patterned mutational or truncation profiles during RT, thereby revealing the precise position of m⁶A (Fig. 2c).

Despite these advances in the detection resolution, the stoichiometry of m⁶A sites remains unclear. In 2013, a method called site-specific cleavage and radioactive-labeling followed by ligation-assisted extraction and thin-layer chromatography (SCARLET) was developed³⁹. This method can quantify m⁶A stoichiometry at specific loci. Recently, a method called m⁶A-level and isoform-characterization sequencing (m⁶A-LAIC-seq) was developed to quantify the m⁶A stoichiometry in a transcriptome-wide fashion⁴⁰. In m⁶A-LAIC-seq, full-length RNAs are used in the m⁶A immunoprecipitation experiments, and an excess of antibody is used to ensure that all m⁶A-containing RNA are pulled down. External RNA Controls Consortium (ERCC) spike ins are added into the input, supernatant and eluate RNA pools as internal standards. The m⁶A levels per gene can be quantified by the ERCC-normalized ratio of RNA abundances in different pools ((eluate)/(eluate + supernatant)) (Fig. 2d). m⁶A-LAIC-seq reveals that

most genes exhibit less than 50% m⁶A-methylation levels; another key finding of the method is that transcripts marked by m⁶A are coupled with proximal alternative polyadenylation sites, resulting in shortened 3' UTRs.

While both single-base and quantitative sequencing technologies for m⁶A have been developed, several challenges still remain. First, although changes of m⁶A stoichiometry of the same site in different samples can be obtained by m⁶A-LAIC-seq, it is currently difficult to compare the methylation levels between different sites in the same transcript because full-length RNA is used in m⁶A-LAIC-seq. Second, it was noted that m⁶A profiling could be heavily impacted by bioinformatics analysis (the choice of peak detection, alignment methods, etc.)³. Hence, caution should always be taken when analyzing and comparing sequencing data (this is also applicable to other RNA modifications). Third, all existing technologies rely on the m⁶A-specific antibodies; yet, it has actually been shown in the yeast study that these antibodies could have intrinsic bias on RNA sequences and secondary structures³⁵. Hence, new methods that are independent of antibodies are still desired.

m⁶Am, at the beginning of an mRNA polynucleotide

m⁶Am is a cap-related modification and occurs at the first nucleotide after the 7-methylguanosine cap⁴¹. When a 2'-O-methyladenosine residue is present in the 'capped' 5' end of mRNA, a methyl group can then be installed on the 2'-O-methyladenosine^{42,43}. As m⁶Am is rec-

ognized by the anti-m⁶A antibody⁴⁴, m⁶A-seq also detects the m⁶Am near the transcription start site (TSS)^{15,19}. In the single-base miCLIP technology, m⁶Am sites can be more precisely identified by detecting crosslinking-induced truncation sites (CITSS) at the 5' UTR³⁸. These truncation sites in 5' UTR tend to occur in BCA (B = C/U/G) motifs rather than in the canonical RRACH motifs for m⁶A. This observation is consistent with the known pyrimidine-rich sequence at TSSs, and it also indicates that these sites are bona fide m⁶Am rather than internal m⁶A. Although the content of m⁶Am in mRNA is approximately 30-fold lower than that of m⁶A (ref. 40) (**Supplementary Table 1**), great care must still be taken to ensure the recognition specificity of the antibody.

m⁵C, more challenging to detect than its DNA counterpart

m⁵dC is a widespread epigenetic marker in DNA and has been extensively studied. m⁵C is also found in abundant noncoding RNAs including tRNA and rRNA¹. In tRNA, m⁵C can stabilize the secondary structure and influence the anticodon stem-loop conformation^{45,46}; in rRNA, m⁵C can affect translational fidelity⁴⁷. Two RNA methyltransferases, NSUN2 and DNMT2, have been identified to catalyze m⁵C methylation in higher eukaryotes^{48,49}.

To detect m⁵dC on DNA, bisulfite treatment has been widely used. However, on account of the significant degradation of nucleic acids during bisulfite treatment, bisulfite-based protocol cannot be directly used for m⁵C detection in RNA. Thus, a modified bisulfite

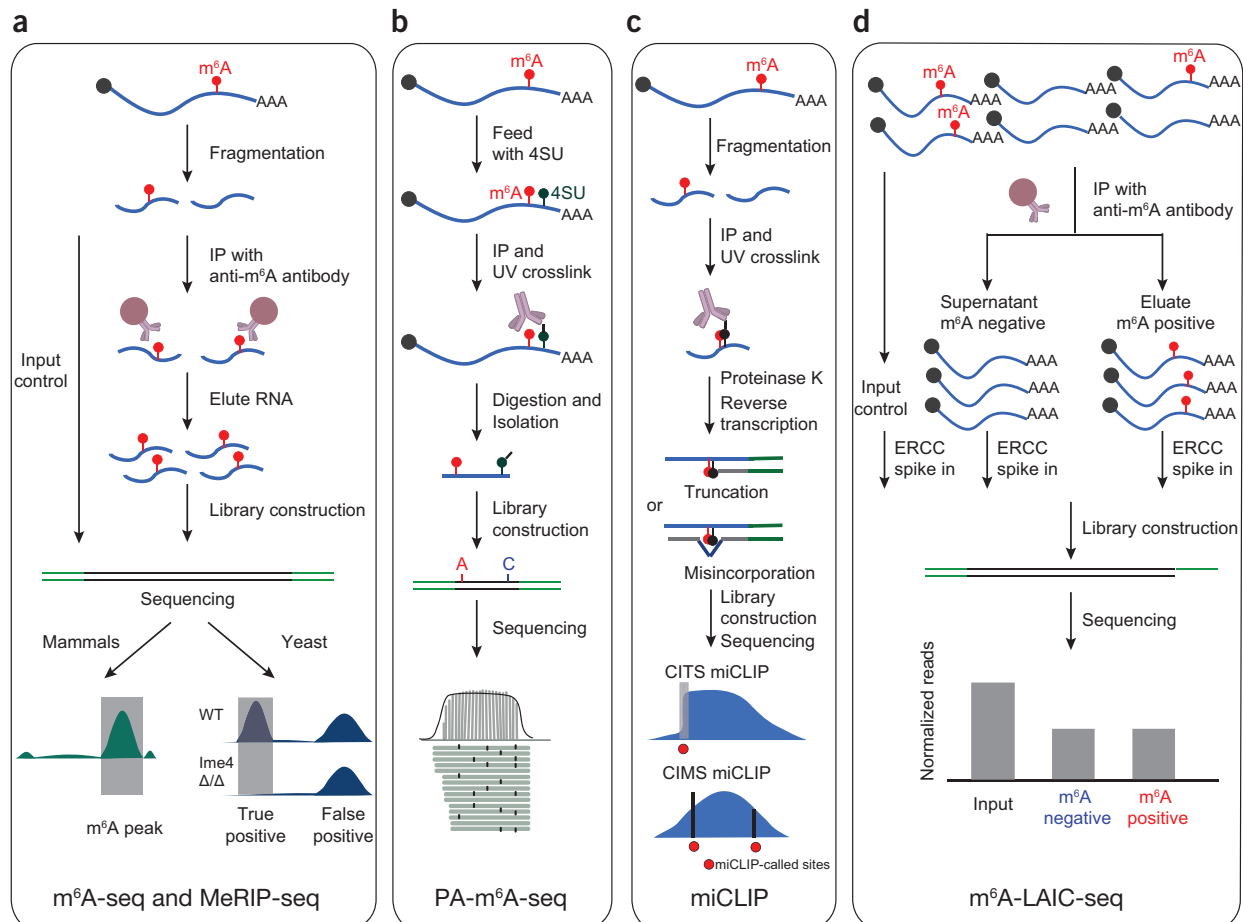


Figure 2 | Transcriptome-wide sequencing methods for m⁶A. (a) m⁶A-seq and MeRIP-seq. WT, wild type. (b) PA-m⁶A-seq. The black bold bars in the figure represent T-to-C transitions induced by 4SU and crosslinking. (c) miCLIP. (d) m⁶A-LAIC-seq.

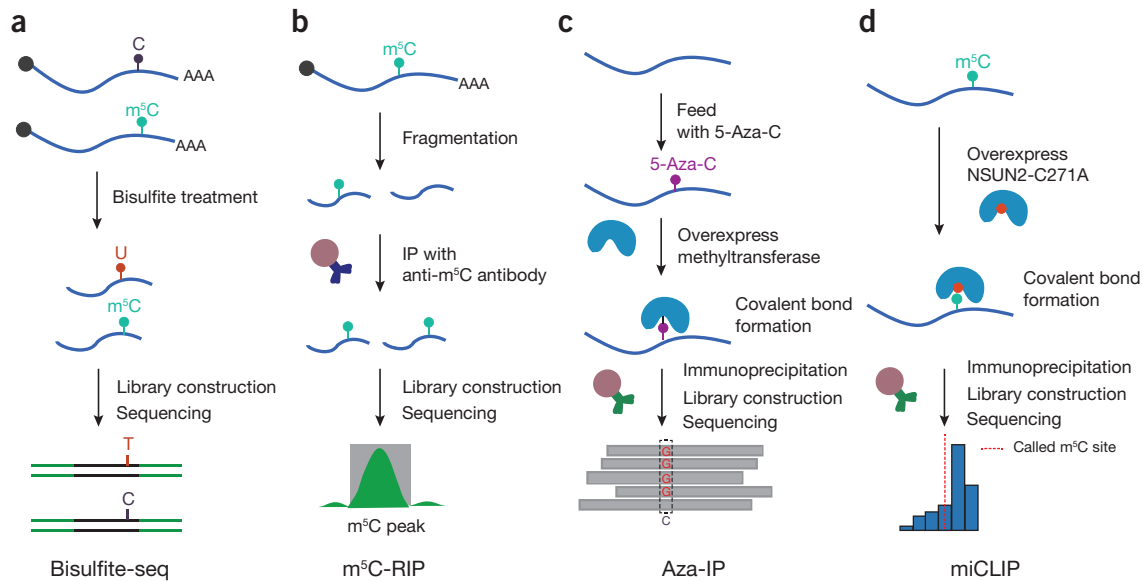


Figure 3 | Detecting m^5C in the transcriptome. (a) Bisulfite-seq. (b) m^5C -RIP. (c) Aza-IP. (d) miCLIP.

treatment protocol was developed; this protocol allows m^5C -site detection in tRNA and rRNA⁵⁰. In 2012, a m^5C methylome was obtained in a transcriptome-wide manner by combining modified bisulfite treatment and high-throughput sequencing⁵¹ (Fig. 3a). This method identified more than 8,000 potential m^5C sites in human mRNA. However, because of the incomplete conversion of regular cytosines in the dsRNA regions and other modifications resistant to bisulfite treatment, others have suggested that these sites include potential false positives^{6,52,53}. Furthermore, because the bisulfite treatment leads to significant RNA degradation and cannot pre-enrich m^5C -containing RNA, this method requires high sequencing depth to detect methylation in low-abundance RNA⁵². In a different study, m^5C sites of *Sulfolobus solfataricus* mRNA identified using bisulfite sequencing have been validated by m^5C RNA immunoprecipitation (m^5C -RIP)⁵⁴ (Fig. 3b).

Recently, two different approaches have been developed to identify the direct targets of the m^5C RNA methyltransferases. One is 5-azacytidine-mediated RNA immunoprecipitation (Aza-IP), which exploits the catalytic mechanisms of the m^5C methyltransferases to covalently link methyltransferase to its RNA targets⁵⁵. First, the cytidine analog 5-azacytidine is randomly incorporated into the nascent RNA of cells overexpressing an epitope-tagged m^5C RNA methyltransferase. Due to the nitrogen substitution at the C5 position, a stable covalent bond forms when the RNA methyltransferase attacks the C6 position of its RNA targets. These targets are enriched by immunoprecipitation and subsequently sequenced (Fig. 3c). In addition, a specific C to G transversion could be observed in the targeted cytosine residue, allowing base-resolution detection of m^5C sites. Using this approach, the direct targets of NSUN2 and DNMT2 have been identified in a transcriptome-wide manner, by two independent experiments⁵⁵. Yet, m^5C sites that are not replaced by 5-azacytidine will be missed in this method. The other approach also exploits the catalytic mechanisms of the m^5C methyltransferase: the cysteine-to-alanine mutation (C271A) in the human NSUN2 protein inhibits the release of the enzyme from the protein–RNA complex, resulting in a stable covalent bond between NSUN2 and its RNA targets⁵⁶. Combining this strategy with CLIP (without UV), the method called miCLIP

(methylation iCLIP) successfully identifies the targets of NSUN2 in the transcriptome⁵⁶ (Fig. 3d). These two approaches can identify the direct targets and are not affected by potential redundancy of different methyltransferases. In addition, the immunoprecipitation procedures allow detection of low-abundance methylated RNAs without the requirement of extremely deep sequencing.

hm^5dC in DNA is generated by oxidation of m^5dC mediated by the TET protein and is now established as an important epigenetic marker^{57,58}. This m^5dC oxidation prompted the question of whether oxidation derivatives of m^5C are present in RNA⁵⁹. In fact, hm^5C was first found in the rRNA of wheat seedlings in 1978 (ref. 60). Recently, both mammalian and *Drosophila* TET proteins have been shown to oxidize m^5C to hm^5C (refs. 61 and 62); isotope-tracing experiments have also demonstrated that m^5C in RNA can be oxidatively metabolized into hm^5C and 5-formylcytidine⁶³ (Supplementary Table 1). In 2016, a method called ‘hMeRIP-seq’, which uses an hm^5C -specific antibody, was developed to map hm^5C in the transcriptome⁶¹. Applying hMeRIP-seq to S2 cells, over 3,000 hm^5C peaks have been identified in the *Drosophila melanogaster* transcriptome⁶¹. Many hm^5C peaks are located in the coding sequences; this distribution pattern is different from that of m^5C (Supplementary Table 1), suggesting that hm^5C and m^5C have different roles. Yet, base-resolution methods for hm^5C detection remain unexplored. For hm^5dC on DNA, two quantitative, base-resolution methods are available^{64,65}. TAB-seq first protects hm^5dC with enzyme-mediated glucosylation, and then uses a TET enzyme to ‘remove’ m^5dC , thereby detecting hm^5dC with bisulfite conversion. oxBS-seq utilizes $KRuO_4$ to selectively oxidize hm^5dC , thereby distinguishing hm^5dC from m^5dC during bisulfite treatment. It remains to be seen whether these methods are suitable for hm^5C detection on RNA, since they rely on bisulfite treatment. In addition, the beta-glucosyltransferase might not work as efficiently in ssRNA as in dsDNA; and $KRuO_4$ -mediated oxidation might react to the 2'-hydroxyl group of ribonucleotides.

Inosine, stringent bioinformatics and orthogonal approaches

Adenosine-to-inosine (A-to-I) editing is the most prevalent type of RNA editing in higher eukaryotes and can be catalyzed by the dsRNA-

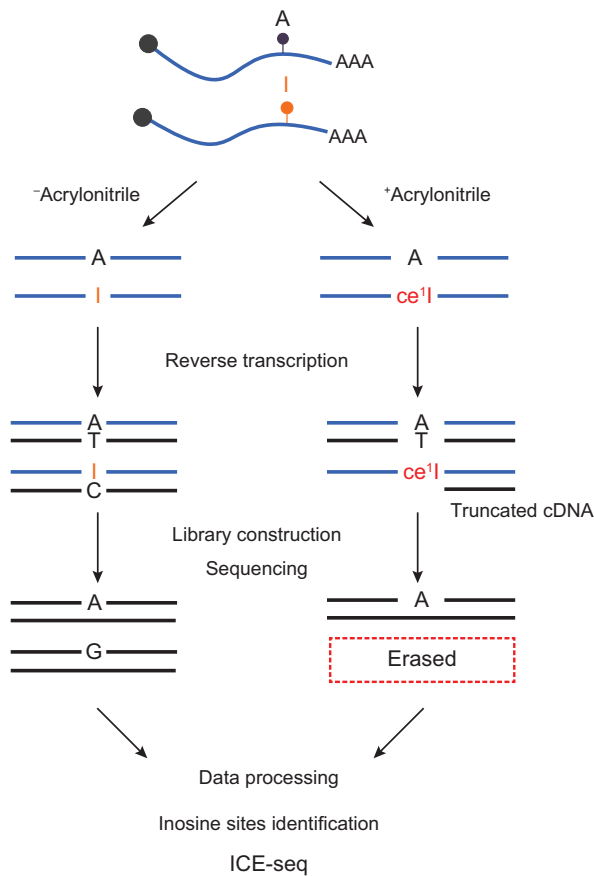


Figure 4 | ICE-seq.

specific adenosine deaminases acting on RNA (ADARs)^{66–68}. ADARs have a preference for dsRNA, and A-to-I editing frequently occurs in *Alu* elements in untranslated regions and introns^{69,70}. A-to-I editing plays numerous roles in modulating gene expression, including recoding codons, altering alternative splicing and regulating miRNA biogenesis and function⁷¹.

Inosine provides one example in which the base-pairing property of the modified base differs from that of the original one. Inosine pairs with cytidine, rather than adenosine, in RT and is thus read as guanosine in cDNA. Hence, one strategy to identify A-to-I editing sites is to detect the A-to-G mismatch sites by analyzing cDNA sequences and the corresponding genomic sequences. The major challenge for this strategy is the background noise caused by single nucleotide polymorphisms (SNPs), somatic mutations, pseudogenes and sequencing errors⁷¹. Thus, initially only sites that are within potential dsRNA regions were considered in order to minimize such noise^{69,70,72}. In 2009, using massively parallel target capture and DNA sequencing, an unbiased method was developed that allowed the identification of ~36,000 editing candidates that are residing outside of the repetitive sequences⁷³. Although the idea of inosine identification by comparing genomic DNA and RNA sequencing data from the same individuals may sound simple, in reality it can be complicated by many factors, including improper bioinformatics^{74–77}. Fortunately, several groups subsequently developed different computational approaches, allowing high-confidence identification of the editing sites in the whole transcriptome^{78–81}. This is a typical example of the paramount importance of strict and robust computational pipelines to the detection of RNA

modifications. More recently, a method that detects inosine sites based only on RNA-seq data from multiple samples has been developed. This method takes advantage of the multitude of publicly available RNA-seq data and thus does not require deep sequencing of both the transcriptome and the genome from the same individual⁸².

As the conventional approach for detecting A-to-G mismatch sites could be complicated by many factors, an alternative chemical labeling method, inosine chemical erasing (ICE), was developed in 2010 (ref. 83). In this approach, acrylonitrile is used to selectively react with inosines in RNA, forming *N*¹-cyanoethylinosine (ce¹I). Because ce¹I stalls RT and results in truncation of the cDNA, inosine-containing RNA is ‘eliminated’, while only unmodified RNA gives rise to full length cDNA. By comparing Sanger sequencing results of treated and untreated RNA samples in parallel, the A-to-I editing sites can be detected. In 2014, the ICE method was further coupled to high-throughput sequencing, giving ICE-seq⁸⁴ (Fig. 4). The ICE-seq method conducts an unbiased genome-wide screening of A-to-I editing sites and has been applied to the transcriptome of the adult human brain. The ICE-seq method is also a good example of using orthogonal technologies to allow high-confidence mapping of RNA modifications of great interest and intense studies.

Pseudouridine, an abundant internal mRNA modification

Ψ, or the fifth nucleotide of RNA, is overall the most abundant modification and is widespread in stable ncRNAs including rRNA, tRNA and snRNA⁸⁵. Ψ is generated via isomerization of uridine, catalyzed by two distinct mechanisms: the RNA-dependent mechanism with the box H/ACA ribonucleoproteins and the RNA-independent mechanism with the ‘stand-alone’ Ψ synthases^{86–88}. In these abundant ncRNAs, Ψ plays important roles in regulating their function. For instance, Ψ is required for proper folding of rRNA and for ensuring its translational fidelity^{89–91}; in tRNA Ψ can stabilize the RNA structure, and in snRNA it can affect snRNP biogenesis and mRNA splicing^{85,88}. Recently, Ψ was also found to be present in mRNA, although the biological function of such mRNA pseudouridylation remains enigmatic. Nevertheless, Ψ is abundant in mammalian mRNA, with a Ψ/U ratio of about 0.2–0.6% in human cells and mouse tissues (Supplementary Table 1).

Compared to uridine, Ψ has an additional hydrogen bond donor and a more stable C–C bond; however, these features do not change the Watson–Crick base pairing property of Ψ, making it impossible to distinguish Ψ from U by direct sequencing. To distinguish Ψ from U, a specific chemical labeling approach was developed⁹², relying on a chemical called *N*-cyclohexyl-*N'*-b-(4-methylmorpholinium) ethylcarbodiimide metho-*p*-toluene-sulfonate (CMCT). As the CMC-Ψ adduct stalls RT and terminates the cDNA one nucleotide 3' to it, this reaction was used to detect Ψ sites in rRNA at single-base resolution in a primer extension assay⁹³. However, the primer extension assay relies on prior knowledge of candidate Ψ-containing regions and is more suited for Ψ detection at specific loci. Recently, several approaches have been developed to map Ψ sites in a transcriptome-wide manner by coupling this selective labeling reaction to high-throughput sequencing^{94–97}. In Ψ-Seq, Pseudo-seq and PSI-seq, fragmented mRNA is reacted with CMCT, and the precise Ψ positions are identified in the transcriptome-wide manner^{94–96} (Fig. 5a). These methods have identified ~50–100 Ψ sites in yeast mRNA and ~100–400 sites in human mRNA. Our group also developed CeU-seq, in which a chemically synthesized CMC derivative, azido-CMC (N₃-CMC), is used. After selective chemical labeling of Ψ, we conjugated a biotin

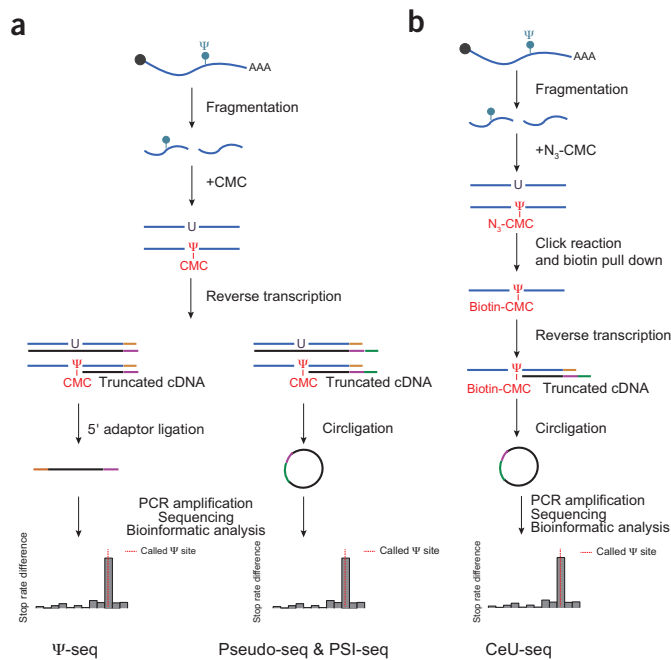


Figure 5 | Transcriptome-wide profiling of Ψ in the eukaryotic cells. (a) Ψ -Seq, PSI-Seq and Pseudo-Seq. (b) CeU-Seq.

molecule to the Ψ -containing RNA, allowing biotin pull-down and pre-enrichment of Ψ -containing RNA before sequencing⁹⁷ (Fig. 5b). Because of the pre-enrichment procedure, Ψ sites of the relative low-abundance mRNA molecules can be detected. Using CeU-seq, thousands of Ψ sites have been identified in the human and mouse transcriptomes.

A previous comparison of mRNA pseudouridylation events in yeast has reported limited overlap among different studies⁹⁸. Instead of re-evaluating the yeast data, we compared the Ψ profiles in the human transcriptome identified by Ψ -seq, Pseudo-seq and CeU-seq. To allow fair comparison, we reanalyzed the sequencing data from the three studies using the same bioinformatics algorithm. We found that the overlap between Ψ -seq and Pseudo-seq data can be readily increased from ~13% (directly using the reported Ψ sites) to ~41%, suggesting the use of different bioinformatics cutoffs could underestimate the overlap between data sets. Moreover, ~51% and ~69% of Ψ sites identified by Ψ -seq and Pseudo-seq, respectively, can be found in the more comprehensive Ψ profiles of CeU-seq. In fact, the use of the same computational standard has also been shown to improve the consistency of m⁶A-seq and MeRIP-seq data³. In addition, it has been shown that mRNA pseudouridylation is tissue specific⁹⁷, hence factors other than bioinformatics algorithms also need to be considered when comparing the profiles of RNA modifications. Three different human cell lines were used by Ψ -seq, Pseudo-seq and CeU-seq; given that there are 13 pseudouridine synthases in mammals, the differential expression pattern of these enzymes in cell lines and tissues is very likely to result in context-dependent pseudouridylation events.

While these first methods successfully reveal the widespread and dynamic nature of mRNA pseudouridylation in eukaryotic cells, several improvements could be made to further enhance transcriptome-wide Ψ profiling. First, all existing methods rely on the RT stops caused by CMC- Ψ adducts to detect Ψ s at single-base resolution. If optimized RT conditions that allow misincorporation-containing readthrough events—instead of RT stops at CMC- Ψ adducts—could

be identified, such mutational profiles could be an alternative strategy for Ψ detection⁹³. Compared to RT stops, readthrough events are expected to make better use of sequencing reads and increase signal-to-noise ratio (by reducing potential bias resulted from fragmentation, ligation and secondary structures). Second, in order to achieve specificity, CMC-mediated labeling of Ψ is neither complete nor quantitative. New chemicals that can react with Ψ more efficiently may allow transcriptome-wide quantification^{99,100}; and such chemicals could also be azido derivatized to further increase the confidence of Ψ detection, similar to the use of both CIMS and/or CITS and m⁶A peaks in miCLIP.

m¹A, new adenosine methylation in eukaryotic mRNA

m¹A is prevalent in tRNA and rRNA¹. In tRNA, m¹A methylation at position 58 is catalyzed by TRMT6 and the TRMT61A complex for cytoplasmic tRNA or by TRMT61B for mitochondrial tRNA^{101,102}; and m¹A methylation plays an important role in stabilizing the tertiary structures of the tRNA molecules¹⁰³. m¹A at position 9 of metazoan mitochondrial tRNA is catalyzed by Trmt10C, and it can affect tRNA structure folding¹⁰⁴. In human 28S rRNA, m¹A is methylated at position 1,322 by RRP8 (also known as NML), and this methylation is necessary for proper rRNA biogenesis^{105,106}.

Compared to regular adenosines, m¹A has an additional methyl group at the Watson–Crick interface. Owing to this structural change, m¹A can not only lead to the generation of truncated cDNAs but can also cause misincorporation at this site in the readthrough cDNAs^{100,105}. However, using such an intrinsic property of m¹A to directly detect the transcriptome-wide location of m¹A will require formidable depth of sequencing and present great challenges for the subsequent bioinformatics analysis. Hence, a pre-enrichment step would be crucial. Early this year, we and others independently reported two technologies (termed ‘m¹A-seq’ and ‘m¹A-ID-seq’) to map the m¹A methylome in the eukaryotic transcriptome^{107,108}. Both methods rely on a very specific m¹A antibody to enrich m¹A-containing RNA, thus combining m¹A immunoprecipitation and high-throughput sequencing. Additional strategies are employed in both methods to further increase the confidence and resolution of detection. For example, m¹A-seq takes advantage of a chemical-assisted reaction to convert the RT-interfering m¹A to the RT-silent m⁶A (ref. 107) (Fig. 6a); while m¹A-ID-seq utilizes an RNA/DNA demethylase to convert m¹A into regular A after immunoprecipitation¹⁰⁸ (Fig. 6b). By comparing the sequencing profiles of the demethylase treated and untreated samples, the high-confidence m¹A peaks can be identified. Despite these technical differences, the main findings by these two technologies very satisfactorily confirm each other. In addition, given the success of antibody-based single-base and quantitative m⁶A sequencing methods, enhanced m¹A sequencing technologies are expected in the near future to further aid our functional investigations of this new epitranscriptomic mark.

Outlook

Despite these major achievements, there is an unmet biological need for new sequencing technologies. First, there is a lack of orthogonal methods to detect the RNA modifications. Second, methods to allow absolute stoichiometry quantification are still needed. Given the identification and importance of different types of differentially methylated regions (DMRs) in DNA, it is tempting to speculate that differentially modified regions in RNA could also be identified. Third, more robust and sensitive methods that need less input are needed not only

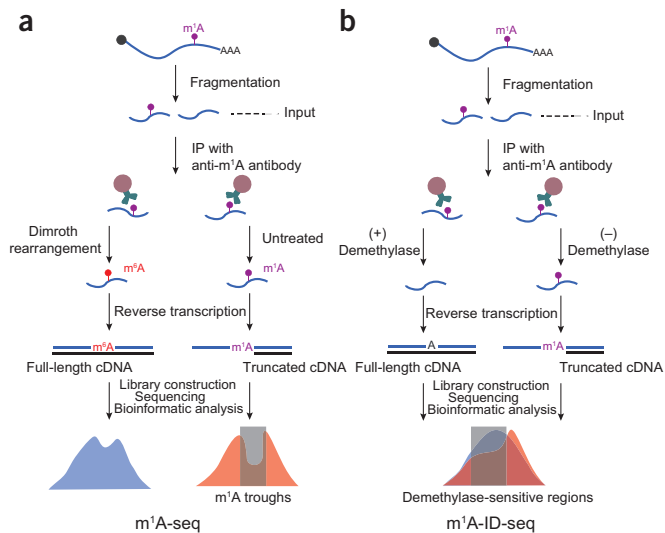


Figure 6 | Mapping the m¹A methylome. (a) m¹A-seq. (b) m¹A-ID-seq.

for biological studies but also for future studies of the physiological roles of the epitranscriptome. Fourth, the spatial relationship of different epitranscriptomic marks within the same transcript is largely unknown. Recently, two single-molecule methods—SMRT sequencing and the Nanopore technology—have demonstrated specific and base-resolution detection of m⁶A in synthetic RNA molecules^{3,109}. These single-molecule approaches could potentially be used to detect multiple RNA modifications simultaneously and to address the challenge of epitranscriptomic phasing problems. Fifth, novel sequencing methods are needed to identify new epitranscriptomic marks in a transcriptome-wide manner. For instance, recent approaches based on alkaline hydrolysis or RT pausing have been reported for the detection of 2'-O-methylation in eukaryotic cells^{110–115}. With further advancement in technology, transcriptome-wide 2'-O-methylation as well as additional RNA modifications could be detected.

Analogous to histone code in which different histone modifications regulate transcription of genetic information, different RNA modifications may regulate the metabolism and function of RNA in a potential 'RNA code'. Despite the recent boom in the field of epitranscriptomics, our current knowledge regarding the epitranscriptome could be just the tip of the iceberg. We envision that future epitranscriptome sequencing technologies will continue to uncover the complexity of the epitranscriptome and enable functional characterization.

Note: Any Supplementary Information and Source Data files are available in the online version of the paper.

ACKNOWLEDGMENTS

We thank all members of the Yi laboratory for their insights and discussions. This work was supported by the National Basic Research Foundation of China (grant nos. MOST2016YFC0900300 and 2014CB964900) and the National Natural Science Foundation of China (grant no. 21522201).

COMPETING FINANCIAL INTERESTS

The authors declare no competing financial interests.

Reprints and permissions information is available online at <http://www.nature.com/reprints/index.html>.

- Machnicka, M.A. *et al.* MODOMICS: a database of RNA modification pathways—2013 update. *Nucleic Acids Res.* **41**, D262–D267 (2013).
- He, C. Grand challenge commentary: RNA epigenetics? *Nat. Chem. Biol.* **6**, 863–865 (2010).

This paper termed the scope and mechanisms of dynamic RNA modifications 'RNA epigenetics' for the first time.

- Saletore, Y. *et al.* The birth of the Epitranscriptome: deciphering the function of RNA modifications. *Genome Biol.* **13**, 175 (2012).

This paper first termed the multitude of RNA modifications as 'epitranscriptome'.

- Fu, Y., Dominissini, D., Rechavi, G. & He, C. Gene expression regulation mediated through reversible m⁶A RNA methylation. *Nat. Rev. Genet.* **15**, 293–306 (2014).
- Liu, N. & Pan, T. N⁶-methyladenosine–encoded epitranscriptomics. *Nat. Struct. Mol. Biol.* **23**, 98–102 (2016).
- Gilbert, W.V., Bell, T.A. & Schaenig, C. Messenger RNA modifications: form, distribution, and function. *Science* **352**, 1408–1412 (2016).
- Meyer, K.D. & Jaffrey, S.R. The dynamic epitranscriptome: N⁶-methyladenosine and gene expression control. *Nat. Rev. Mol. Cell Biol.* **15**, 313–326 (2014).
- Lee, M., Kim, B. & Kim, V.N. Emerging roles of RNA modification: m(6)A and U-tail. *Cell* **158**, 980–987 (2014).
- Saletore, Y., Chen-Kiang, S. & Mason, C.E. Novel RNA regulatory mechanisms revealed in the epitranscriptome. *RNA Biol.* **10**, 342–346 (2013).
- Bokar, J.A., Rath-Shambaugh, M.E., Ludwiczak, R., Narayan, P. & Rottman, F. Characterization and partial purification of mRNA N⁶-adenosine methyltransferase from HeLa cell nuclei. Internal mRNA methylation requires a multisubunit complex. *J. Biol. Chem.* **269**, 17697–17704 (1994).
- Liu, J. *et al.* A METTL3–METTL14 complex mediates mammalian nuclear RNA N⁶-adenosine methylation. *Nat. Chem. Biol.* **10**, 93–95 (2014).
- Wang, Y. *et al.* N⁶-methyladenosine modification destabilizes developmental regulators in embryonic stem cells. *Nat. Cell Biol.* **16**, 191–198 (2014).
- Bokar, J.A., Shambaugh, M.E., Polayes, D., Matera, A.G. & Rottman, F.M. Purification and cDNA cloning of the AdoMet-binding subunit of the human mRNA (N⁶-adenosine)-methyltransferase. *RNA* **3**, 1233–1247 (1997).
- Ping, X.L. *et al.* Mammalian WTAP is a regulatory subunit of the RNA N⁶-methyladenosine methyltransferase. *Cell Res.* **24**, 177–189 (2014).
- Schwartz, S. *et al.* Perturbation of m⁶A writers reveals two distinct classes of mRNA methylation at internal and 5' sites. *Cell Reports* **8**, 284–296 (2014).
- Jia, G. *et al.* N⁶-methyladenosine in nuclear RNA is a major substrate of the obesity-associated FTO. *Nat. Chem. Biol.* **7**, 885–887 (2011).

This work discovered the first m⁶A RNA demethylase ('eraser')—FTO, demonstrating reversible RNA methylation in the human transcriptome.

- Zheng, G. *et al.* ALKBH5 is a mammalian RNA demethylase that impacts RNA metabolism and mouse fertility. *Mol. Cell* **49**, 18–29 (2013).
- Alarcón, C.R. *et al.* HNRNPA2B1 is a mediator of m(6)A-dependent nuclear RNA processing events. *Cell* **162**, 1299–1308 (2015).
- Dominissini, D. *et al.* Topology of the human and mouse m⁶A RNA methylomes revealed by m⁶A-seq. *Nature* **485**, 201–206 (2012).

This is an important study that reports the first m⁶A methylome in the mammalian transcriptome.

- Liu, N. *et al.* N(6)-methyladenosine-dependent RNA structural switches regulate RNA–protein interactions. *Nature* **518**, 560–564 (2015).
- Meyer, K.D. *et al.* 5' UTR m(6)A promotes cap-independent translation. *Cell* **163**, 999–1010 (2015).
- Wang, X. *et al.* N⁶-methyladenosine-dependent regulation of messenger RNA stability. *Nature* **505**, 117–120 (2014).
- Wang, X. *et al.* N(6)-methyladenosine modulates messenger RNA translation efficiency. *Cell* **161**, 1388–1399 (2015).
- Xiao, W. *et al.* Nuclear m(6)A reader YTHDC1 regulates mRNA splicing. *Mol. Cell* **61**, 507–519 (2016).
- Lichinchi, G. *et al.* Dynamics of the human and viral m(6)A RNA methylomes during HIV-1 infection of T cells. *Nat. Microbiol.* **1**, 16011 (2016).
- Tirumuru, N. *et al.* N(6)-methyladenosine of HIV-1 RNA regulates viral infection and HIV-1 Gag protein expression. *eLife* **5**, e15528 (2016).
- Gokhale, N.S. *et al.* N⁶-methyladenosine in *Flaviviridae* viral RNA genomes regulates infection. *Cell Host Microbe* **20**, 654–665 (2016).
- Kennedy, E.M. *et al.* Posttranscriptional m(6)A editing of HIV-1 mRNAs enhances viral gene expression. *Cell Host Microbe* **19**, 675–685 (2016).
- Lichinchi, G. *et al.* Dynamics of human and viral RNA methylation during zika virus infection. *Cell Host Microbe* **20**, 666–673 (2016).
- Desrosiers, R., Friderici, K. & Rottman, F. Identification of methylated nucleosides in messenger RNA from Novikoff hepatoma cells. *Proc. Natl. Acad. Sci. USA* **71**, 3971–3975 (1974).
- Csepány, T., Lin, A., Baldick, C.J. Jr. & Beemon, K. Sequence specificity of mRNA N⁶-adenosine methyltransferase. *J. Biol. Chem.* **265**, 20117–20122 (1990).
- Narayan, P. & Rottman, F.M. An *in vitro* system for accurate methylation of internal adenosine residues in messenger RNA. *Science* **242**, 1159–1162 (1988).
- Narayan, P., Ludwiczak, R.L., Goodwin, E.C. & Rottman, F.M. Context effects on N⁶-adenosine methylation sites in prolactin mRNA. *Nucleic Acids Res.* **22**, 419–426 (1994).

34. Meyer, K.D. *et al.* Comprehensive analysis of mRNA methylation reveals enrichment in 3' UTRs and near stop codons. *Cell* **149**, 1635–1646 (2012).
The other study that first reports the transcriptome-wide m⁶A methylome.
35. Schwartz, S. *et al.* High-resolution mapping reveals a conserved, widespread, dynamic mRNA methylation program in yeast meiosis. *Cell* **155**, 1409–1421 (2013).
36. Chen, K. *et al.* High-resolution N(6)-methyladenosine (m(6)A) map using photo-crosslinking-assisted m(6)A sequencing. *Angew. Chem. Int. Edn Engl.* **54**, 1587–1590 (2015).
37. Ke, S. *et al.* A majority of m6A residues are in the last exons, allowing the potential for 3' UTR regulation. *Genes Dev.* **29**, 2037–2053 (2015).
38. Linder, B. *et al.* Single-nucleotide-resolution mapping of m6A and m6Am throughout the transcriptome. *Nat. Methods* **12**, 767–772 (2015).
39. Liu, N. *et al.* Probing N6-methyladenosine RNA modification status at single nucleotide resolution in mRNA and long noncoding RNA. *RNA* **19**, 1848–1856 (2013).
40. Molin e, B. *et al.* m(6)A-LAIC-seq reveals the census and complexity of the m(6)A epitranscriptome. *Nat. Methods* **13**, 692–698 (2016).
41. Schibler, U. & Perry, R.P. The 5'-termini of heterogeneous nuclear RNA: a comparison among molecules of different sizes and ages. *Nucleic Acids Res.* **4**, 4133–4149 (1977).
42. Keith, J.M., Ensinger, M.J. & Mose, B. HeLa cell RNA (2'-O-methyladenosine-N6-)-methyltransferase specific for the capped 5'-end of messenger RNA. *J. Biol. Chem.* **253**, 5033–5039 (1978).
43. Wei, C., Gershowitz, A. & Moss, B. N6, O2'-dimethyladenosine a novel methylated ribonucleoside next to the 5' terminal of animal cell and virus mRNAs. *Nature* **257**, 251–253 (1975).
44. Munns, T.W., Oberst, R.J., Sims, H.F. & Liszewski, M.K. Antibody-nucleic acid complexes. Immunospecific recognition of 7-methylguanine- and N6-methyladenine-containing 5'-terminal oligonucleotides of mRNA. *J. Biol. Chem.* **254**, 4327–4330 (1979).
45. Motorin, Y. & Helm, M. tRNA stabilization by modified nucleotides. *Biochemistry* **49**, 4934–4944 (2010).
46. Squires, J.E. & Preiss, T. Function and detection of 5-methylcytosine in eukaryotic RNA. *Epigenomics* **2**, 709–715 (2010).
47. Chow, C.S., Lamichhane, T.N. & Mahto, S.K. Expanding the nucleotide repertoire of the ribosome with post-transcriptional modifications. *ACS Chem. Biol.* **2**, 610–619 (2007).
48. Brzezicha, B. *et al.* Identification of human tRNA:m5C methyltransferase catalysing intron-dependent m5C formation in the first position of the anticodon of the pre-tRNA Leu (CAA). *Nucleic Acids Res.* **34**, 6034–6043 (2006).
49. Goll, M.G. *et al.* Methylation of tRNA^{Asp} by the DNA methyltransferase homolog Dnmt2. *Science* **311**, 395–398 (2006).
50. Schaefer, M., Pollex, T., Hanna, K. & Lyko, F. RNA cytosine methylation analysis by bisulfite sequencing. *Nucleic Acids Res.* **37**, e12 (2009).
51. Squires, J.E. *et al.* Widespread occurrence of 5-methylcytosine in human coding and non-coding RNA. *Nucleic Acids Res.* **40**, 5023–5033 (2012).
52. Hussain, S., Aleksic, J., Blanco, S., Dietmann, S. & Frye, M. Characterizing 5-methylcytosine in the mammalian epitranscriptome. *Genome Biol.* **14**, 215 (2013).
53. Shafik, A., Schumann, U., Evers, M., Sibbritt, T. & Preiss, T. The emerging epitranscriptomics of long noncoding RNAs. *Biochim. Biophys. Acta* **1859**, 59–70 (2016).
54. Edelheit, S., Schwartz, S., Mumbach, M.R., Wurtzel, O. & Sorek, R. Transcriptome-wide mapping of 5-methylcytidine RNA modifications in bacteria, archaea, and yeast reveals m5C within archaeal mRNAs. *PLoS Genet.* **9**, e1003602 (2013).
55. Khoddami, V. & Cairns, B.R. Identification of direct targets and modified bases of RNA cytosine methyltransferases. *Nat. Biotechnol.* **31**, 458–464 (2013).
56. Hussain, S. *et al.* NSun2-mediated cytosine-5 methylation of vault noncoding RNA determines its processing into regulatory small RNAs. *Cell Reports* **4**, 255–261 (2013).
57. Kriaucionis, S. & Heintz, N. The nuclear DNA base 5-hydroxymethylcytosine is present in Purkinje neurons and the brain. *Science* **324**, 929–930 (2009).
58. Tahiliani, M. *et al.* Conversion of 5-methylcytosine to 5-hydroxymethylcytosine in mammalian DNA by MLL partner TET1. *Science* **324**, 930–935 (2009).
59. Li, S. & Mason, C.E. The pivotal regulatory landscape of RNA modifications. *Annu. Rev. Genomics Hum. Genet.* **15**, 127–150 (2014).
60. R acz, I., Kir aly, I. & L asztlly, D. Effect of light on the nucleotide composition of rRNA of wheat seedlings. *Planta* **142**, 263–267 (1978).
61. Delatte, B. *et al.* RNA biochemistry. Transcriptome-wide distribution and function of RNA hydroxymethylcytosine. *Science* **351**, 282–285 (2016).
62. Fu, L. *et al.* Tet-mediated formation of 5-hydroxymethylcytosine in RNA. *J. Am. Chem. Soc.* **136**, 11582–11585 (2014).
63. Huber, S.M. *et al.* Formation and abundance of 5-hydroxymethylcytosine in RNA. *ChemBioChem* **16**, 752–755 (2015).
64. Booth, M.J. *et al.* Quantitative sequencing of 5-methylcytosine and 5-hydroxymethylcytosine at single-base resolution. *Science* **336**, 934–937 (2012).
65. Yu, M. *et al.* Base-resolution analysis of 5-hydroxymethylcytosine in the mammalian genome. *Cell* **149**, 1368–1380 (2012).
66. Nishikura, K. Functions and regulation of RNA editing by ADAR deaminases. *Annu. Rev. Biochem.* **79**, 321–349 (2010).
67. Bass, B.L. RNA editing by adenosine deaminases that act on RNA. *Annu. Rev. Biochem.* **71**, 817–846 (2002).
68. Jepson, J.E. & Reenan, R.A. RNA editing in regulating gene expression in the brain. *Biochim. Biophys. Acta* **1779**, 459–470 (2008).
69. Levanon, E.Y. *et al.* Systematic identification of abundant A-to-I editing sites in the human transcriptome. *Nat. Biotechnol.* **22**, 1001–1005 (2004).
70. Athanasiadis, A., Rich, A. & Maas, S. Widespread A-to-I RNA editing of *Alu*-containing mRNAs in the human transcriptome. *PLoS Biol.* **2**, e391 (2004).
71. Wulff, B.E., Sakurai, M. & Nishikura, K. Elucidating the inosinome: global approaches to adenosine-to-inosine RNA editing. *Nat. Rev. Genet.* **12**, 81–85 (2011).
72. Kim, D.D. *et al.* Widespread RNA editing of embedded *Alu* elements in the human transcriptome. *Genome Res.* **14**, 1719–1725 (2004).
73. Li, J.B. *et al.* Genome-wide identification of human RNA editing sites by parallel DNA capturing and sequencing. *Science* **324**, 1210–1213 (2009).
74. Li, M. *et al.* Widespread RNA and DNA sequence differences in the human transcriptome. *Science* **333**, 53–58 (2011).
75. Lin, W., Piskol, R., Tan, M.H. & Li, J.B. Comment on “Widespread RNA and DNA sequence differences in the human transcriptome”. *Science* **335**, 1302–e (2012).
76. Pickrell, J.K., Gilad, Y. & Pritchard, J.K. Comment on “Widespread RNA and DNA sequence differences in the human transcriptome”. *Science* **335**, 1302–d (2012).
77. Kleinman, C.L. & Majewski, J. Comment on “Widespread RNA and DNA sequence differences in the human transcriptome”. *Science* **335**, 1302–c (2012).
78. Ju, Y.S. *et al.* Extensive genomic and transcriptional diversity identified through massively parallel DNA and RNA sequencing of eighteen Korean individuals. *Nat. Genet.* **43**, 745–752 (2011).
79. Bahn, J.H. *et al.* Accurate identification of A-to-I RNA editing in human by transcriptome sequencing. *Genome Res.* **22**, 142–150 (2012).
80. Ramaswami, G. *et al.* Accurate identification of human *Alu* and non-*Alu* RNA editing sites. *Nat. Methods* **9**, 579–581 (2012).
81. Peng, Z. *et al.* Comprehensive analysis of RNA-Seq data reveals extensive RNA editing in a human transcriptome. *Nat. Biotechnol.* **30**, 253–260 (2012).
82. Ramaswami, G. *et al.* Identifying RNA editing sites using RNA sequencing data alone. *Nat. Methods* **10**, 128–132 (2013).
83. Sakurai, M., Yano, T., Kawabata, H., Ueda, H. & Suzuki, T. Inosine cyanoethylation identifies A-to-I RNA editing sites in the human transcriptome. *Nat. Chem. Biol.* **6**, 733–740 (2010).
84. Sakurai, M. *et al.* A biochemical landscape of A-to-I RNA editing in the human brain transcriptome. *Genome Res.* **24**, 522–534 (2014).
85. Karij lich, J., Yi, C. & Yu, Y.T. Transcriptome-wide dynamics of RNA pseudouridylation. *Nat. Rev. Mol. Cell Biol.* **16**, 581–585 (2015).
86. Kiss, T., Fayet-Lebaron, E. & J ady, B.E. Box H/ACA small ribonucleoproteins. *Mol. Cell* **37**, 597–606 (2010).
87. Hama, T. & Ferr e-D'Amar e, A.R. Pseudouridine synthases. *Chem. Biol.* **13**, 1125–1135 (2006).
88. Li, X., Ma, S. & Yi, C. Pseudouridine: the fifth RNA nucleotide with renewed interests. *Curr. Opin. Chem. Biol.* **33**, 108–116 (2016).
89. Decatur, W.A. & Fournier, M.J. rRNA modifications and ribosome function. *Trends Biochem. Sci.* **27**, 344–351 (2002).
90. Baudin-Baillieu, A. *et al.* Nucleotide modifications in three functionally important regions of the *Saccharomyces cerevisiae* ribosome affect translation accuracy. *Nucleic Acids Res.* **37**, 7665–7677 (2009).
91. Jack, K. *et al.* rRNA pseudouridylation defects affect ribosomal ligand binding and translational fidelity from yeast to human cells. *Mol. Cell* **44**, 660–666 (2011).
92. Gilham, P.T. An addition reaction specific for uridine and guanosine nucleotides and its application to the modification of ribonuclease action. *J. Am. Chem. Soc.* **84**, 687–688 (1962).
93. Bakin, A. & Ofengand, J. Four newly located pseudouridylation residues in *Escherichia coli* 23S ribosomal RNA are all at the peptidyltransferase center: analysis by the application of a new sequencing technique. *Biochemistry* **32**, 9754–9762 (1993).

94. Schwartz, S. *et al.* Transcriptome-wide mapping reveals widespread dynamic-regulated pseudouridylation of ncRNA and mRNA. *Cell* **159**, 148–162 (2014). **This work reports Ψ-seq to map Ψ sites in the yeast and human transcriptome.**
95. Carlile, T.M. *et al.* Pseudouridine profiling reveals regulated mRNA pseudouridylation in yeast and human cells. *Nature* **515**, 143–146 (2014). **This study reports Pseudo-seq to map Ψ sites in the yeast and human transcriptome.**
96. Lovejoy, A.F., Riordan, D.P. & Brown, P.O. Transcriptome-wide mapping of pseudouridines: pseudouridine synthases modify specific mRNAs in *S. cerevisiae*. *PLoS One* **9**, e110799 (2014).
97. Li, X. *et al.* Chemical pulldown reveals dynamic pseudouridylation of the mammalian transcriptome. *Nat. Chem. Biol.* **11**, 592–597 (2015). **This study reports CeU-Seq for the comprehensive identification of Ψ sites in the human and mouse transcriptome.**
98. Zaringhalam, M. & Papavasiliou, F.N. Pseudouridylation meets next-generation sequencing. *Methods* **107**, 63–72 (2016).
99. Kellner, S., Burhenne, J. & Helm, M. Detection of RNA modifications. *RNA Biol.* **7**, 237–247 (2010).
100. Behm-Ansmant, I., Helm, M. & Motorin, Y. Use of specific chemical reagents for detection of modified nucleotides in RNA. *J. Nucleic Acids* **2011**, 408053 (2011).
101. Ozanick, S., Krecic, A., Andersland, J. & Anderson, J.T. The bipartite structure of the tRNA m1A58 methyltransferase from *S. cerevisiae* is conserved in humans. *RNA* **11**, 1281–1290 (2005).
102. Chujo, T. & Suzuki, T. Trmt61B is a methyltransferase responsible for 1-methyladenosine at position 58 of human mitochondrial tRNAs. *RNA* **18**, 2269–2276 (2012).
103. Schevitz, R.W. *et al.* Crystal structure of a eukaryotic initiator tRNA. *Nature* **278**, 188–190 (1979).
104. Vilardo, E. *et al.* A subcomplex of human mitochondrial RNase P is a bifunctional methyltransferase—extensive moonlighting in mitochondrial tRNA biogenesis. *Nucleic Acids Res.* **40**, 11583–11593 (2012).
105. Hauenschild, R. *et al.* The reverse transcription signature of N-1-methyladenosine in RNA-Seq is sequence dependent. *Nucleic Acids Res.* **43**, 9950–9964 (2015).
106. Waku, T. *et al.* NML-mediated rRNA base methylation links ribosomal subunit formation to cell proliferation in a p53-dependent manner. *J. Cell Sci.* **129**, 2382–2393 (2016).
107. Dominissini, D. *et al.* The dynamic N(1)-methyladenosine methylome in eukaryotic messenger RNA. *Nature* **530**, 441–446 (2016). **This study reports the transcriptome-wide m¹A methylome for the first time.**
108. Li, X. *et al.* Transcriptome-wide mapping reveals reversible and dynamic N(1)-methyladenosine methylome. *Nat. Chem. Biol.* **12**, 311–316 (2016). **This work reports the transcriptome-wide m¹A methylome for the first time.**
109. Garalde, D.R. *et al.* Highly parallel direct RNA sequencing on an array of nanopores. Preprint at <http://biorxiv.org/content/early/2016/08/12/068809> (2016).
110. Dong, Z.W. *et al.* RTL-P: a sensitive approach for detecting sites of 2'-O-methylation in RNA molecules. *Nucleic Acids Res.* **40**, e157 (2012).
111. Lacoux, C. *et al.* BC1-FMRP interaction is modulated by 2'-O-methylation: RNA-binding activity of the tudor domain and translational regulation at synapses. *Nucleic Acids Res.* **40**, 4086–4096 (2012).
112. Birkedal, U. *et al.* Profiling of ribose methylations in RNA by high-throughput sequencing. *Angew. Chem. Int. Edn Engl.* **54**, 451–455 (2015).
113. Gumienny, R., Jedlinski, D., Martin, G., Vina-Villaseca, A. & Zavolan, M. High-throughput identification of C/D box snoRNA targets with CLIP and RiboMeth-seq. Preprint at <http://biorxiv.org/content/early/2016/01/19/037259> (2016).
114. Incarnato, D. *et al.* High-throughput single-base resolution mapping of RNA 2'-O-methylated residues. *Nucleic Acids Res.* **Sup 9**, gkw810 (2016).
115. Marchand, V., Blanloeil-Oillo, F., Helm, M. & Motorin, Y. Illumina-based RiboMethSeq approach for mapping of 2'-O-Me residues in RNA. *Nucleic Acids Res.* **44**, e135 (2016).

Erratum: Epitranscriptome sequencing technologies: decoding RNA modifications

Xiaoyu Li, Xushen Xiong & Chengqi Yi

Nat. Methods 14, 23–31 (2017); published online 29 December 2017; corrected after print 10 February 2017

In the version of this article initially published, author affiliation numbers were incorrect. Xiaoyu Li originally had affiliation 1; this has been changed to affiliations 1 and 2. Xushen Xiong originally had affiliations 1 and 2; these have been changed to affiliations 1–3. Chengqi Yi originally had affiliations 1 and 3; these have been changed to affiliations 2 and 4. The error has been corrected in the HTML and PDF versions of the article.